Asian Journal of Nanoscience and Materials, 2019, 2(2), 120-130.

FULL PAPER

Synthesis and Characterization of Noble Metal Nanowires by Electrodeposition in Porous Anodic Alumina Membranes

Ahmed Alya'a Jabbar

Directorate of Scholarship and Cultural Relations, Ministry of Higher Education and Scientific Research, Baghdad-Iraq.

Received: 29 September 2018, Revised: 14 November 2018 and Accepted: 07 December 2018.

ABSTRACT: Electrochemical deposition is a very efficient method for producing many types of modern materials. This method is not expensive and does not have a limit for sample size. In our work, the preparation of Ag and Au nanowires is presented. The obtained nanowires had different diameter and length, which were tunable by template porous material and time of deposition, respectively. The quality of the prepared wires was dependent also on deposition mode. The smallest wires of the diameter around 29 nm were prepared in porous anodic alumina oxide obtained from sulfuric acid. The largest ones, around 44 nm, were produced in oxalic acid. The morphology and surface structure of the AAO films were examined before and after electrodeposition by scanning electron microscopy (SEM), atomic force microscope (AFM), and x-ray diffraction spectroscopy.

KEYWORDS: AAO template; Ag nanowires; Au nanowire; Metal- phenothiazine complex.

GRAPHICAL ABSTRACT:

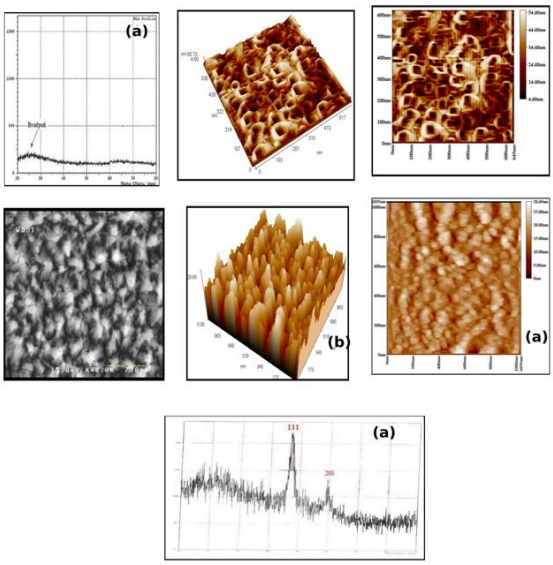

1. Introduction

A great deal of thought has been paid as of late to nanostructured materials as they show novel physical and chemical properties. This is especially valid for metallic nanostructures. Efforts in both essential research and creation have energized the utilization of these materials in different novel applications including the fields of detecting [1], catalysis [2], optics [3], electronics [4], and surface-enhanced Raman scrambling (SERS) [5]. It has been recommended that anodic aluminum oxide (AAO) layers are ideal for design controlled creation [6] in light of the fact that they have the accompanying attractive attributes: controllable pore sizes (both diameter and length), high thermal stability and great mechanical strength. While a scope of all around -developed deposition have just

*Corresponding author: Alya'a Jabbar Ahmed, E-mail: alyaa.jabbar@yahoo.com , Tel: +964 7709648903

Asian Journal of Nanoscience and Materials

been utilized to manufacture nanostructures (e.g. . Electrochemical deposition [7], electroless deposition [8], chemical vapor deposition [9] and physical evaporation [10]), electrodeposition has ended up being a minimal effort and high return method for producing large arrays of nanowires. It is especially valuable for creating nanowires from various materials, with distances across less than100 nm[11]. Possible templates incorporate nuclear track- etched polycarbonate layers, nanochannel cluster glasses, mesoporous channel hosts, and self-requested anodized aluminum oxide AAO films. It has been discovered that AAO is steady at high temperature and in natural solvents and that the pore directs in AAO films are uniform, parallel, and opposite to the layer surface [12]. This makes AAO films perfect formats for the electrodeposition of nanowire clusters. AAO films have already been utilized as formats to blend an assortment of metal and semiconductor nanowires through electrochemical procedures [13]. Be that as it may, the nanowire clusters which came about because of the vast majority of the electrodeposition forms have shown the alleged "high rise" marvel related to an absence of length consistency and control. Normal to these procedures is the utilization of fluid arrangements, except for a not many that utilized natural arrangements [14].

2. Experimental

2.1. Preparation of AAO membranes

High-purity aluminum sheets (99.98%) with a thickness of 0.2 mm were cut into 32mm in diameter circle was employed in our experiment to fabricate the AAO template. The Al sheets were first annealed at 500 ˚C for 2 h, degreased using acetone and ethanol, then rinsed in distilled water. The Al sheets were electropolished in a mixture of $HClO_4$and C_2H_5OH (1:4v/v) for 4 min. The polished Al sheets were anodized in 5 wt% H_2SO_4 at 20 V, 20 ˚C or 0.3 M $H_2C_2O_4$ at 40 V , 0 ˚C. The sheets anodization were usually carried out for 30 min. Subsequently, the anodized Al sheets were put into an acid mixture (6 wt% H_3PO_4 and 1.8 wt% CrO_3) to completely remove the porous layer. Then, the second anodization was conducted for 2 h at the same conditions as the first anodization. The barrier layers were then removed by 5 wt% H_3PO_4 at 20 ˚C for 10 minutes.

2.2. Preparation of Ag and Au nanowires

Metal-phenothiazine complex under-investigated was synthesized as follows: (0.169 gm,1mmole) of silver nitrate dissolved in 5ml of absolute ethanol was added drop by drop to (0.199gm,1mmole) of the ligand (phenothiazine) dissolved in 15ml of dimethylformamide, the resulting formation complex having violet color. In case gold-phenothiazine complex (0.35 gm,1mmole) of chloronic acid monohydrate dissolved in 5ml of absolute ethanol was added drop by drop to (0.39gm,2mmole) of the ligand(phenothiazine) dissolved in 15ml of dimethylformamide, the resulting formation complex having brown color Electrodeposition of Ag and Au nanowires were carried out at room temperature on the AAO without removing its back (cathode) the silver silk and Pt foil served as an anode for the Ag and Au deposition respectively. Freshly prepared metals-phenothiazine, complex as electrolytic solutions. The pore size of the AAO membrane and the metal nanowires were examined using a Scanning Electron Microscope (SEM, 54700, Hitachi). And Atomic Force Microscope (AFM, AA3000, Angstrom). The crystallographic structures of the samples were identified using an X-ray Diffractometer (XRD- 6000 with Cu-K, wave 1.5A, 40 kV, 30 mA) at a scanning step size of 2θ =0.05º in the 2θ range from 20º to 60º. Identification and study of the

Asian Journal of Nanoscience and Materials

metal complex were carried out by percentage of metal analysis using AA-680 Shimadzu Atomic Absorption Spectrophotometer. The electronic spectra of the prepared complex were recorded on a Shimadzu Uv-160 Spectrophotometer. FTIR spectra of the sample were recorded using IR Prestige-21Spectrophotometer.

3. Results and discussion

3.1. Formation and characterization of AAO templates

3.1.1. Electrical current

The electrical current passing through the apparatus was measured throughout the second anodization of the Al sample. Figures (1 a and b) show the current density–time characteristics for second anodization in sulfuric and oxalic acid, under constant operation voltage 20, 40 respectively. The rapid drop of the current density at the beginning indicates the growth of barrier layer, while the process of the steep increase to the maxima current density corresponds to the pore nucleation and formation, and a nearly exponential decrease to the pore channel elongation [15]. It was found that the current for oxalic as anodic agent Figure (1 a) is almost twice of that for sulfuric acid as anodic agent Figure (1 b), where the operating voltage for the first case is twice of that in the second case. Due to the imperfection of the aluminum plate surface, the configuration of the alumina pore got some defects.

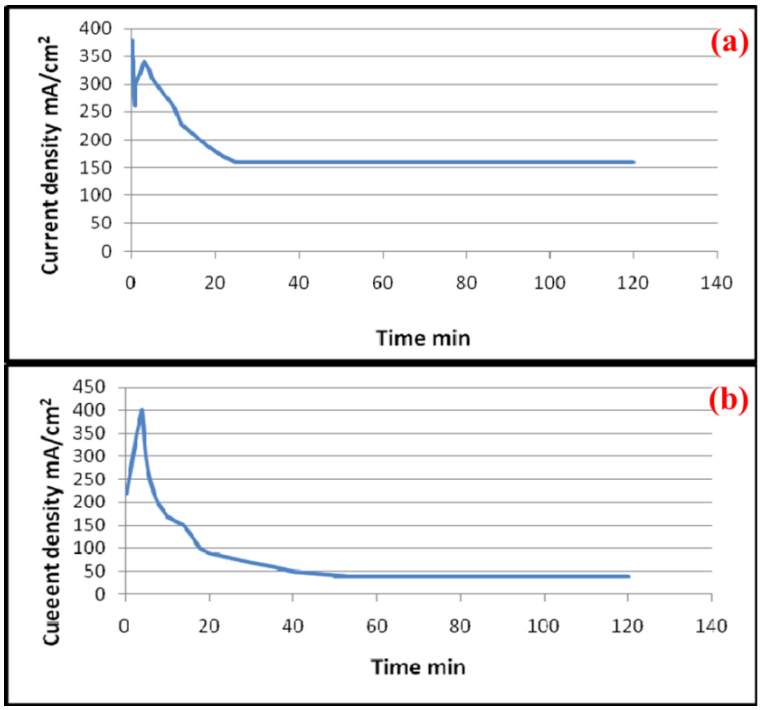

Fig. 1. The current density–time characteristic of AAO films anodized in different acids (a) oxalic acid, (b) sulfuric acid.

3.1.2. AFM analysis

Various electrolytes determine the diameter of the pores and the degree of ordering. According to the report of the pore diameter-acid relationship, Figures (2 and 3) show the differences of the AAO morphology of AAO obtained with sulfuric and oxalic acid. Figure (2 a) shows well-ordered pores at the surface of the alumina template which was obtained in 5% sulfuric acid under 20˚C and 20 V for 2h. Figure (2 b) demonstrates the 3-D AFM

Asian Journal of Nanoscience and Materials

image of the sample. AFM images are presented in this Figure. Pores with the diameter around (29 nm). Figure (3) shows typical AFM Top-view of AAO nanopores, which was obtained in 0.3 M oxalic acid under 0˚C and 40 V for 2h. Both the 2D (a) and the 3D (b) morphology confirm the successful formation of AAO nanopores. The pore diameter is about 48 nm.

3.1.3. XRD spectroscopy

The XRD pattern of the AAO film shows only a broad peak located in the 2θ angle range of (20-30 ˚C) indicating that AAO film is composed of amorphous alumina Figure (4 a) no sign of contamination with Al metal [16]. Figure (4 b) presents the XRD spectrum of AAO template which was obtained in 0.3 M oxalic acid under 0 ˚C and 40V for 2h. It can be seen the spectrums of AAO have a non-spiculate diffraction peak at 2θ = 20-30° in spectrums indicate the amorphous alumina. The other three diffraction peaks at 2θ = 45.0 3°, 65.41°, and 78.51° are well coincident with the substructure aluminum.

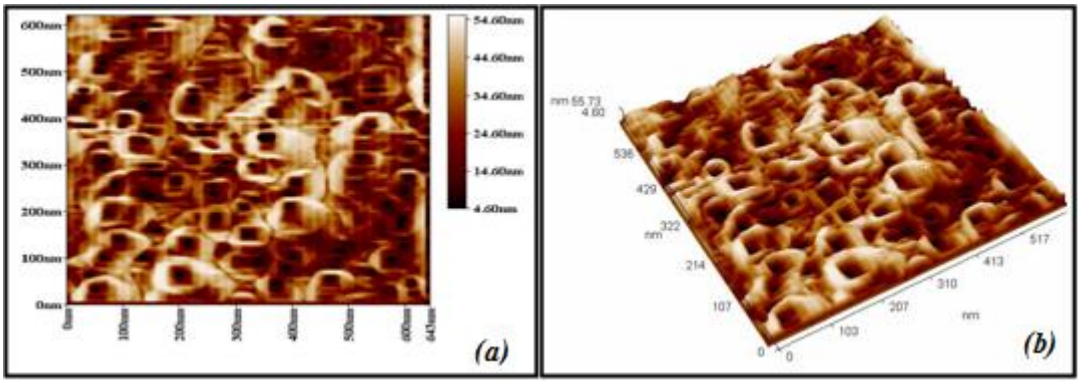

Fig. 2. AFM image of AAO nanoporous obtained in 5% sulfuric acid under 20 ˚C and 20 V for 2h (a) 2D, (b), 3D.

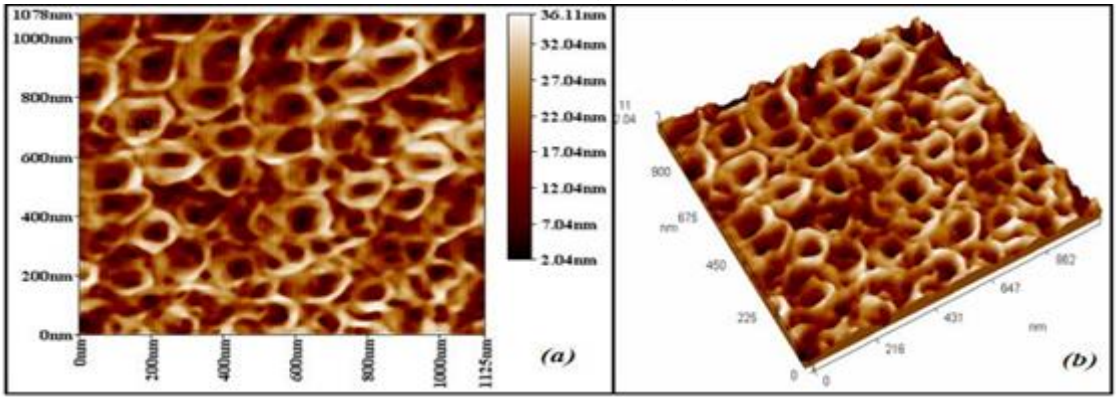

Fig. **3**. AFM image of AAO nanoporous fabricated under 0˚C, 40V for 2h in0. 3 M oxalic acid (a) 2D (b) 3D.

Asian Journal of Nanoscience and Materials

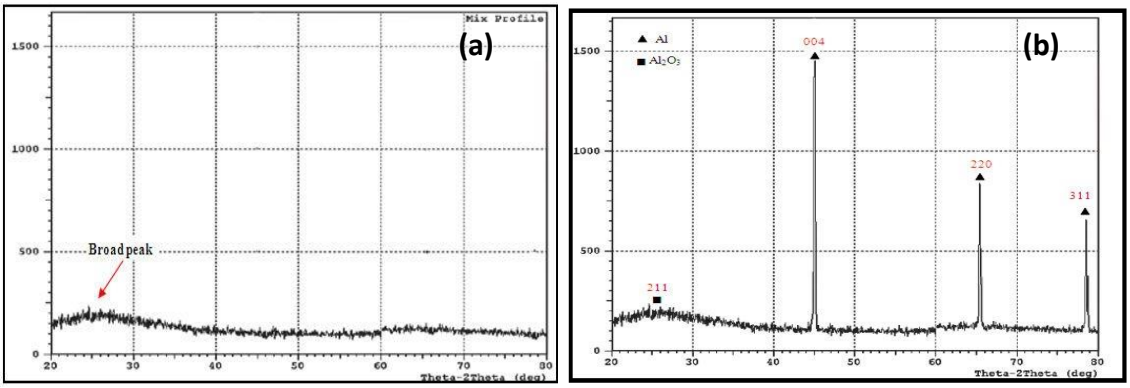

Fig. **4**. XRD of AAO template (a) anodized in sulfuric acid, (b) anodized in oxalic acid.

3.2. Ag, Au Nanowires Fabrication

3.2.1. Spectroscopic Characterization of Silver and Gold-Phenothaiozine complexes

Silver and Gold-Phenothaiozine complexes were freshly prepared to be used as a fuel to fabricate the Ag and Au nanowire via electrodeposition procedure, FTIR, UV-visible, and atomic absorption spectroscopy were conducted to examine the electronic structures of this complex. The results revealed the following suggested structures: $[AgL\ (H_2O)_2]\ NO_3.H_2O$ and $[AuL_2Cl_2]\ Cl.H_2O$.

As expected, The qualitative differences between the infrared spectrum of the free ligand (phenothiazine) Figure (5) and infrared spectra of its metal ion complexes which are shown in Figures (6) and (7) and discussed in order to ascertain ligand to metal ion bonding modes. The infrared spectra of the ligand and its metal ions complexes had indicated presence of weak bands at the (3055-3097 cm^{-1}) [17] which are attributed to the stretching vibration of *ν* (C-H) aromatic and confirmed by the appearance of bending vibration band of ð(C-H) at (1307 -1311 cm^{-1}) . A sharp band at (3340 cm^{-1} and 1597 cm^{-1}) [18] are assigned to the heterocyclic (C-N-C), the (N-H) stretching and bending vibration in the free ligand are shifted to (3236 and 1573 cm^{-1}) [19] in to the spectra of Ag (I) confirming coordination through nitrogen atom to the metal in these complex . The shifting to lower wave number is due to the donation of the lone pair of the electron from the nitrogen atom to metal ion which has a partially filled d-orbital ,this increases the electron positivity of the nitrogen atom and depresses the electron density of the – bonding namely (C=C band) which lowering the wave number . The sharp and medium band in the free ligand at 1118cm^{-1} is assigned to the heterocyclic (C-S-C)[20] vibration in the free ligand, which is confirmed by the appearance of weak to medium intensity band assigned at 1307 cm^{-1} bending vibration, these bands shifted to lower frequency and appeared at (1107 cm^{-1}) and for Au (III) complex confirming the coordination of the ligand through heterocyclic S atom to the metal center Au (III) metal ion. The spectra of studied complexes show abroad bands in the (3549 and 3452cm^{-1}) for Ag and Au complexes respectively assigned to the ð (OH), suggesting the presences of water molecules in the complex structure[21].In the infrared spectra of the complexes a very weak new absorption bands observed at 459 and

Asian Journal of Nanoscience and Materials

408cm^{-1}[22] attributed to Ag-N and Au-S, vibration ,this bands provides an evidence to the coordination through nitrogen atom to the silver (I) metal ion ,where gold(III), metal ion coordinated with the ligand through sulfur atom.

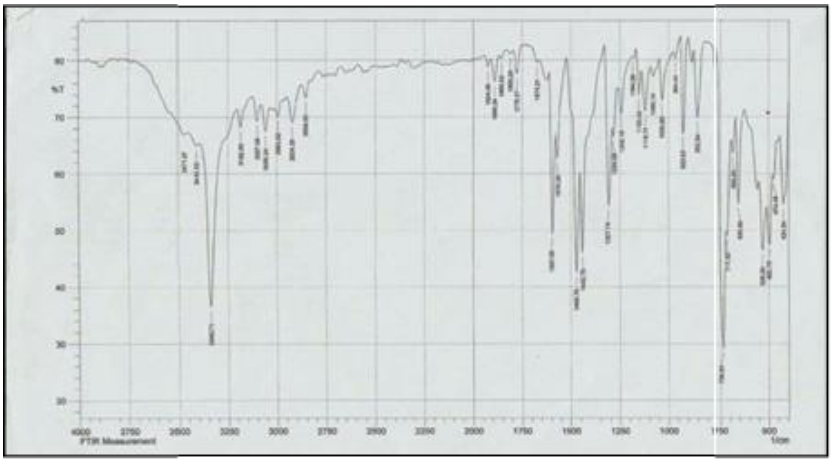

Fig. 5. FT-IR spectrum of L.

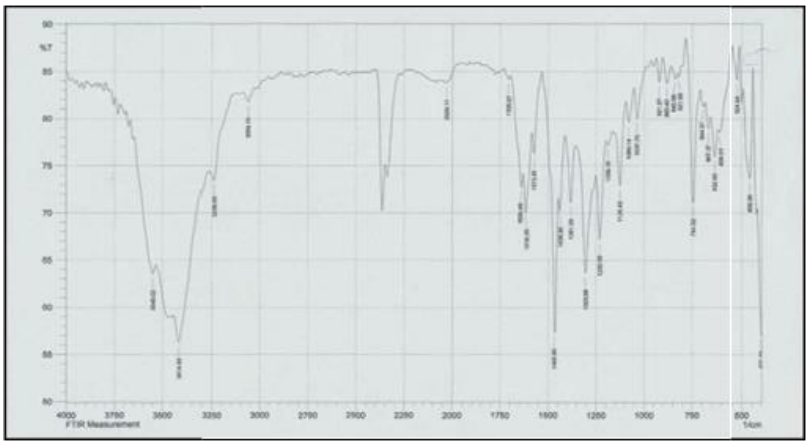

Fig. 6. FT-IR spectrum of AgL.

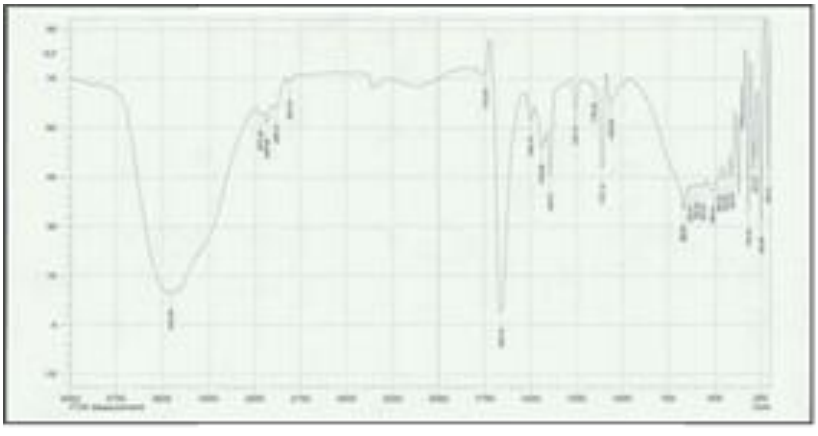

Fig. 7. FT-IR spectrum of AuL.

The electronic spectrum of phenothiazine ligand in (UV-Vis) region in DMF exhibited

Asian Journal of Nanoscience and Materials

in one main band as shown in Figure (8). The absorption band appeared at 319 nm (31347.96) cm^{-1} due to inter-ligand ($\pi \rightarrow \pi^*$) transition may arise from charge transfer. The spectrum of $[AgL(H_2O)_2]NO_3.H_2O$ complex Figure (9) shows bands at 418, 320, and 288nm; the latter band may arise from charge transfer [23]. Conductivity measurement in DMF shows that the complexes were ionic, in addition to these data and that obtained from atomic absorption analysis, infrared spectra, which shows the complex to be conducted, a trigonal geometry around Ag(I). Gold (III) complex is in high crystal field effect due to the large size of gold (III) ion, being in the third transition series in addition to the high oxidation state of this ion. Therefore, spectra of such ions are characterized by charge transfer bands, which dominate the ligand filed transition. This means that the charge transfer bands appear at a longer wavelength; at the same time ligand filed transition is expected to appear at a shorter wavelength. This results in an overlap between the two absorption bands, which make the interpretation of the spectra more difficult [24,25]. In this work, the gold complex showed three bands Figure (10) one at (27322.40) cm^{-1} which refer to ^1A_1g ^1Eg transition and the other appeared at (26737.96) cm^{-1} which refer to ^1A_1g ^1B_1g in a square planar geometry. The band at (32467.90) cm^{-1} may be due to charge transfer.

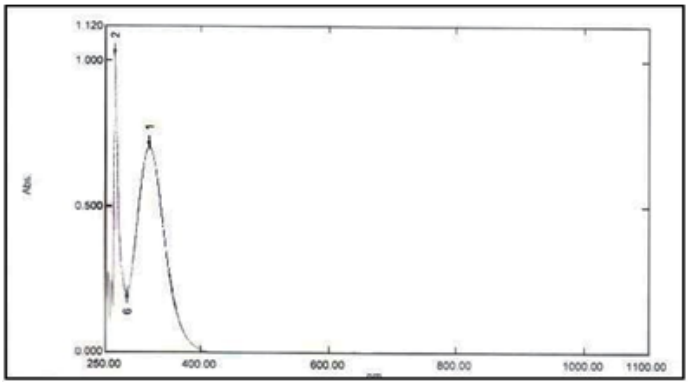

Fig. 8. Electronic Spectrum of L.

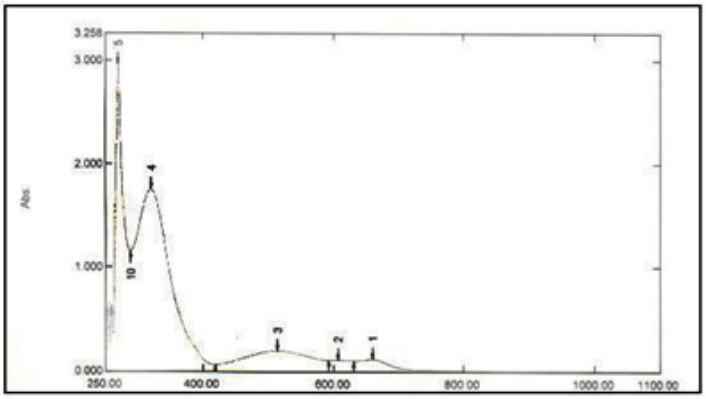

Fig.9. *Electronic Spectrum of AgL.*

Asian Journal of Nanoscience and Materials

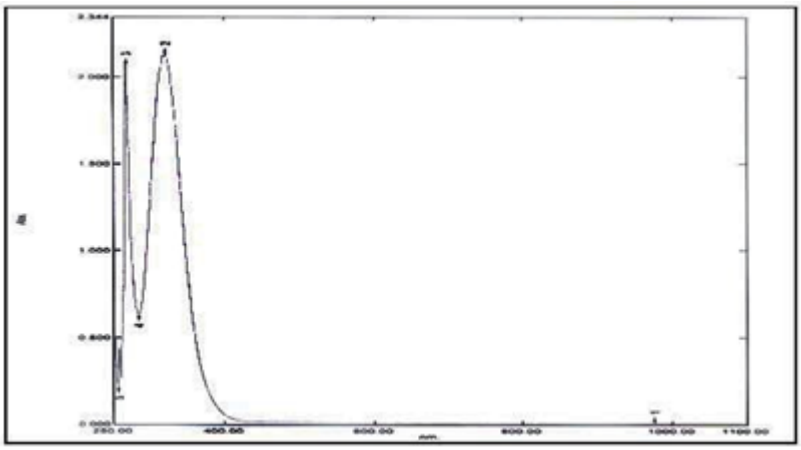

Fig.10. *Electronic Spectrum of AuL.*

3.2.2. AFM analysis of Ag and Au nanowire

AFM micrograph of Ag and Au nanowire is shown in Figure(11)and (12). It can find out that the abundant and free defect nanowires have been prepared. The diameter of the nanowires is about 29nm and 44nm for Ag and Au respectively and approximately equal to those of the nanopores of AAO template used in our experiments**.**

3.2.3. SEM analysis of Ag and Au nanowire array

The filled alumina templates were examined by scanning electron microscopy SEM to determine the degree of pore filling and the extension of the silver nanowires. By etching the filled porous structure from the top, nanowires ending somewhat below the membrane surface became observable for scanning electron microscopy SEM examination. Figure (13) shows two top view micrographs and one side view micrograph of a highly ordered alumina pore structure filled with silver. The pore diameter is approximately 33 nm and the length of the wire is(120) nm. Figure (14) shows the SEM image of gold nano-wire arrays fabricated by template synthesis method. Each gold wire has an average diameter of (39) nm. The average distance between two wires is about (40) nm.

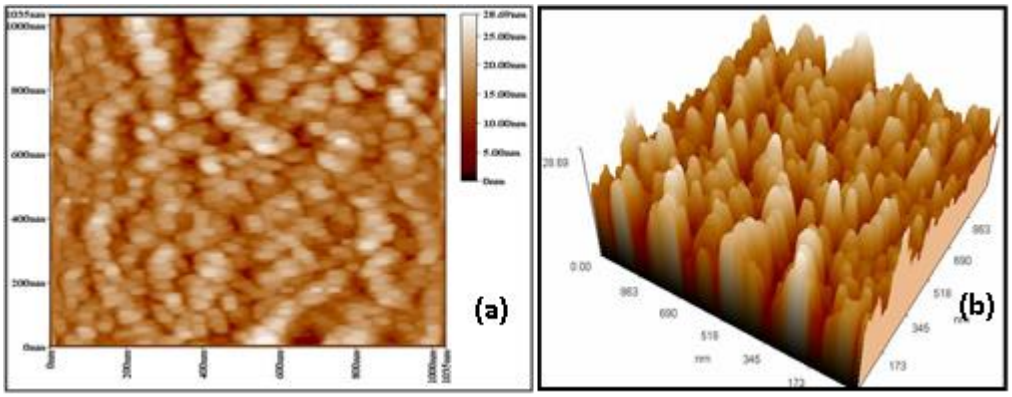

Fig. 11. AFM top image of silver nanowires array grown on the surface of AAO membrane: (a) 2D (b) 3D**.**

Asian Journal of Nanoscience and Materials

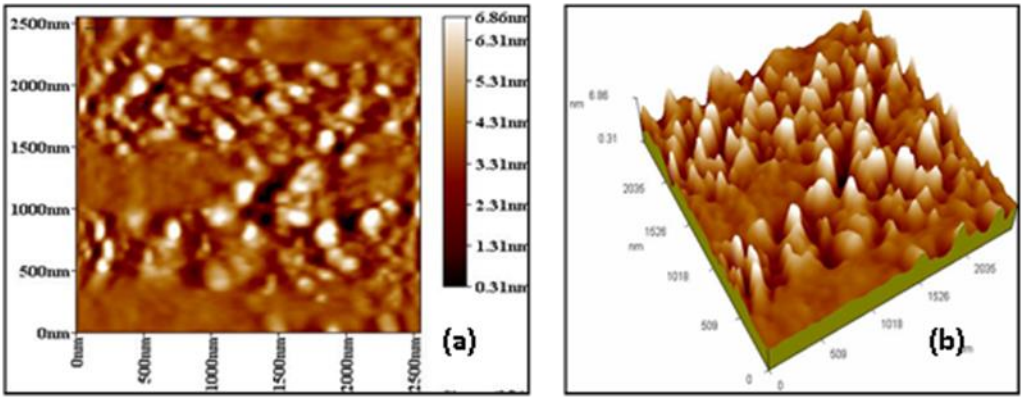

Fig. 12. AFM top image of gold nanowires array grown on the surface of an AAO membrane: (a) 2D, (b) 3D.

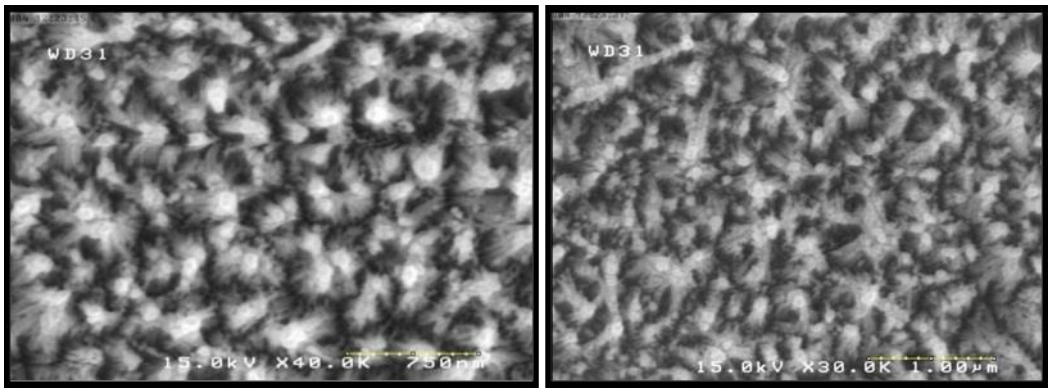

Fig. 13. SEM images of Ag nanowires synthesized with the AAO template.

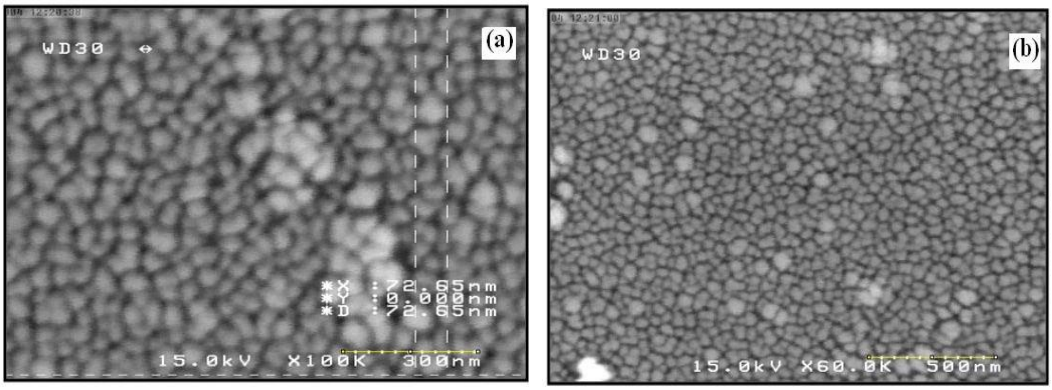

Fig. 14. SEM images of Au nanowires synthesized with the AAO template.

3.2.4. XRD analysis of Ag and Au nanowire arrays

Figure (15 a) shows the XRD pattern of resulting silver nanowires prepared in AAO membranes. The Figure confirms that the silver nanowires possessed a face-centered cubic (FCC) structure and were well crystallized. The diffraction peaks at 2θ =38.51, 44.81, are assigned as the (1 1 1), (2 00) reflection lines, respectively, of the FCC phase of silver. The sharp peaks are good evidence of silver nanowires with high crystallinity. However, the broadening background curve results from the amorphous AAO membrane[26]. XRD measurement Figure (15 b) confirms that the resultant products embedded in the AAO template are

Asian Journal of Nanoscience and Materials

crystalline gold with face-centered cubic (FCC) lattice structure[27].

4. Conclusion:

In summary, electrodeposition directly in the AAO template is a simple and efficient method to produce noble metals Au and Ag nanowire arrays.SEM, AFM, and XRD results demonstrated that these Au and Ag nanowires have a uniform length and diameter. Furthermore, this electrodeposition approach offers the obvious advantage that the deposition of particles starts at the aluminum cathode on the bottom of the nanopores and the length of Ag and Au nanowires can be easily controlled by the deposition time , we believe that this approach offers a new cell and convenient route to fabricate metal Ag and Au wires arrays and may find potential application in fuel sensing devices and so on.

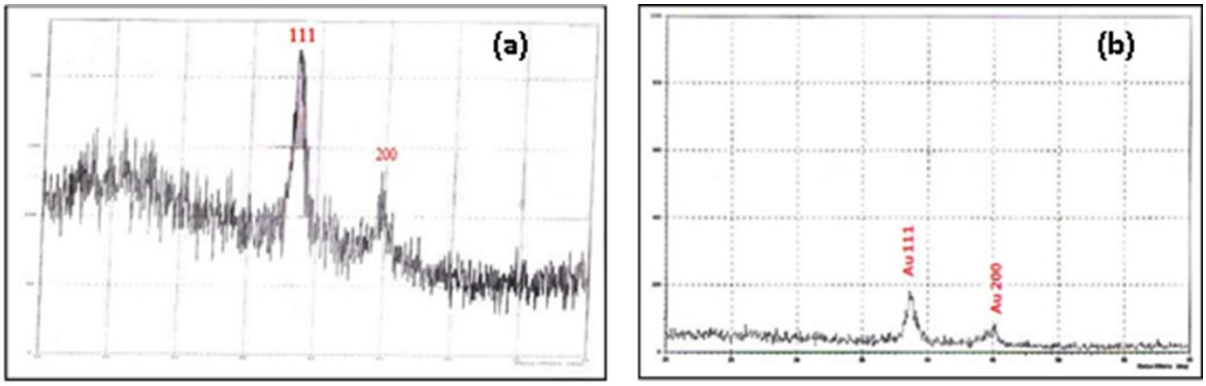

Figure 15: XRD spectra of silver nanowires (**a**), gold nanowires (**b**) prepared in an AAO membrane. The measurement was performed without removing the AAO membranes.

References

1. S.Cattarin, D. Kramer, A.Lui, M.M. Musiani (**2007**) J. Phys. Chem. **34**:12643-12649.
2. X. Teng, D. Black, N J. Watkins, Y. Gao , H. Yang (**2003**) Nano Lett. **3**:261–264.
3. S R. Nicewarner-Peña, R. G. Freeman, B D. Reiss, L. He, D. J. Peña, I. D. Walton, R. Cromer, Christine D. Keating, M J. Natan(**2001**)Science, **294**:137–141.
4. P V. Kamat (**2002**) J. Phys. Chem. B , **106**: 7729-7744.
5. L A. Dick, A D. McFarland, C L. Haynes, R P. Van Duyne (**2002**) J. Phys. Chem. B,**106**: 853–860.
6. JH. Fang, P. Spizzirri , A.Cimmino ,S. Rubanov , S.Prawer (**2009**) Nanotechnology, **20**: 065706.
7. J. Yin, J. Li, W. Jian, A. J. Bennett, J. M. Xu (**2001**) Appl. Phys. Lett. **79**:1039.
8. J.Ahmed, A. M. Alsammarraie, W. A.Mahmmood .Lambert Academic Publishing (**2012**).
9. W. A.Mahmmood, A. M. Alsammarraie, A. J.Ahmed (**2013**) Asian J. Chem.,**25**: 4035-4038.
10. W. Lee, M. Alexe, K. Nielsch, U. Gösele (**2005**) Chem. Mater.,**17**: 3325–3327.
11. K. Ounadjela, R. Ferré, L. Louail, J. M. George, J. L. Maurice, L. Piraux ,S. Dubois (**1997**) Journal of Applied Physics **81**: 5455.

Asian Journal of Nanoscience and Materials

12. O. Jessensky, F. Mu¨ller, U. Go¨sele (**1998**) Appl. Phys. Lett., **72**: 1173-1175.
13. Y. Peng, HL.Zhang, SL. Pan, HL.Li (**2000**) Journal of Applied Physics **87**:7405.
14. D.Xu,Y.Xu,D.Chen,G.Guo,L.Gui,Y. Tang(**2000**) Chemical Physics Letters, **325**: 340-344.
15. Y. Li, M. Zheng, L.Ma, W.Shen. (**2006**) Nanotechnology **17**: 5101–5105.
16. J.H.Yuan,W.Chen,R.J.Hui,Y.L.Hu, X.H.Xia (**2006**) Electrochimica Acta, **51**: 4589-4595.
17. M.Alias,A.M.Seewan,C.Shakir,F.I. Mohammad (**2014**) Int.J Pharm.,**4**:126-132.
18. A.M.Hammam,M.A.,ElGhanami,Z. A.,Khafagi,M.S.Alsalimi,S.A.,Ibrahim(**2015**)J.Mater.Environ.Sci.,**6**:1596-1602.
19. H.K.Jabur, M. F. Alias, T. A. Kareem (**2012**) Baghdad Science J.,**9**: 511-520.
20. M.F.Alias, D. H. Mahal (**2013**) IJSR., **6**: 1469- 1476.
21. M.F.Alias,M.O.Hamza,T.A.Kareem (**2011**) J.of AlNahrain University,**4**:10-18.
22. M.Alias,H.Kassum,C.Shakir(**2013**) JKSUS.,**25**:157-166.
23. J.Ahmed and A. M. Alsammarraie, (**2018**) Asian J. Chem.,**30**: 1608-1612.
24. B.N. Figgis, M. A. Hitchman "Ligand Field Theory And its Application" (**2000**) Wiley-VCH, New York, Singapore, Toronto.
25. Mohamed, I. Kani, A. O. Ramirez, J. P. Fackler (**2004**) Inorg. Chem.,**43**:3833–3839.
26. W.-B. Zhao, J.-J. Zhu, and H.-Y. Chen (**2003**) Journal of Crystal Growth, **258**:176– 180.
27. Q. Xu, G.Meng, X. Wu, Q. Wei, M. Kong, X. Zhu, Z. Chu (**2009**) hem. Mater., **21**: 2397–2402.

How to cite this manuscript: Ahmed Alya'a Jabbar*. Synthesis and Characterization of Noble Metal Nanowires by Electrodeposition in Porous Anodic Alumina Membranes. Asian Journal of Nanoscience and Materials, 2019, **2**(2), 120-130. DOI: 10.26655/ajnanomat.2019.3.1